Effect of gas composition on CMS Cathode Strip Chamber performance

C. Anderson[a], V.Barashko[b], S. Korenblit[b], A. Korytov[b], G. Mitselmakher[b]

[a]*Department of Physics, Luther College, Decorah, Iowa 52101*
[b]*Department of Physics, University of Florida, Gainesville, Florida 32611*

(7/30/2003)

Abstract

Cathode strip chambers (CSCs) are multiwire proportional counters that will be used as muon detectors in the Compact Muon Solenoid (CMS) experiment at the European Center for Nuclear Research (CERN). The composition of the gas inside the chamber influences important chamber parameters, such as gas gain and operational voltage range. Differences in these parameters were examined under variations in concentration of argon, carbon dioxide, and carbon tetrafluoride around the baseline mixture of Ar + CO_2 + CF_4 = 40 + 50 + 10. Gas gain was found to be dependent on Ar concentration, but independent of CF_4 or CO_2 relative concentration. Operational voltage range of ~370V has no dependence on Ar concentration in the range of 60%-40% Ar, and has a weak dependence on the amount of CF_4 (at fixed 40% Ar): ~340V at 0% CF_4 to ~430V at 20% CF_4.

Introduction

Particle Physics

Particle physics is a branch of physics dealing with the most fundamental constituents of matter and the most fundamental forces with which particles interact. Its ultimate goal is to produce a theory that can explain all forces and all qualities of matter.

Currently, the most advanced theory that can describe interactions between particles is the so-called Standard Model. This theory can describe interactions between fundamental particles using two forces – the strong nuclear force, and the electro weak force (a unified electromagnetic and weak nuclear force). Gravity has not been incorporated into this model. The theory uses six quarks of three different "colors" each and six leptons (and their antiparticles) as the constituents of matter.

This theory lacks a great deal in its description of the world – it cannot explain the origin of the masses of its fundamental particles, and the masses cannot be added by hand. In order to correct this problem, an extension to the model was devised which would require the existence of a new particle – the Higgs Boson, which would couple with the particles through a new force, and thus effectively give them mass.

Particle Accelerators

This is where experimental particle physics comes into play. Particle accelerators will be used to accelerate and collide charged particles, such as protons, into each other, and create new particles. According to theory, at a high enough energy of collision some new phenomenon must appear. The simplest phenomenon is the creation of the Higgs boson. The Higgs boson is predicted to have a very short lifetime; only its decay products can be detected.

However, so far the Higgs boson has not been detected in existing colliders. The most powerful collider that exists today, the Tevatron in Chicago, has only a faint possibility of producing Higgs bosons in detectable quantities. This is one of the reasons a new, more powerful collider is being built – the Large Hadron Collider (LHC).

The factors that are important for colliders to have the ability to create new particles in detectable amounts are the energy and luminosity of the beams. Multiplying luminosity by the cross section for the interaction will produce the rate of interactions, which is desired to be high. A high rate of interactions will produce more rare interactions, like the creation of the Higgs boson. The Tevatron has an energy of collision of 2 TeV and a luminosity of 10^{32} $cm^{-2}s^{-1}$, compared to the LHC, which has an energy of collision of 14 TeV and a luminosity of 10^{34} $cm^{-2}s^{-1}$. LHC will have two detectors (out of a total of four) that will be dedicated to finding the Higgs boson, among other things. These detectors are called ATLAS and CMS (Compact Muon Solenoid).

Detectors

Detectors are designed to analyze interactions between particles. They analyze the interactions by identifying the particles created in the collisions by their momentum, and the types of interactions that they have with the matter in the detectors. In order to accomplish this, the detectors are built in onion-like layers. Each layer performs a different function. Some layers block out particles of one type in order to discern what type they are when they do not register in the detectors of the next level. The detector is cylindrical and built around the beam pipe through which the accelerated particles travel and in which they collide (in the center of the detector).

The layers are ordered so that particles are first tracked, then their momentum is measured, and then their energy is measured. The layers have to be ordered so that no particle is absorbed in the material of the detector before it is analyzed. One of the layers has to be a solenoidal magnet that creates a uniform electric field in the tracker, causing the charged particles to have a curved track from which their momentum can be calculated.

Usually, the first layer is a tracking layer that can record where each charged particle first passed. This information is later used to analyze the origin of the particles detected and categorized. The second layer is an electromagnetic calorimeter in which electrons and photons will be absorbed and their energy measured.

The third layer is the hadronic calorimeter. It measures the energy of strongly interacting particles called hadrons, which are composed of quarks. As the hadrons interact with copper in this layer, they form showers of hadrons. These hadrons, as they pass through the interleaving scintillator layers, produce photons, whose overall light intensity is proportional to the magnitude of the hadrons' energy.

The fourth layer is the muon detector. Only muons can reach this layer, so although the detector can detect any charged particle, it can be assumed that the particles detected at this level are muons. Other particles that reach this layer are neutrinos, which can only be accounted for by missing total momentum and energy, since they rarely interact with matter.

Muon Chambers

The muons are of high importance in the CMS detector, since they could possibly indicate that a Higgs Boson was created in the collision, with almost no background. One of the detectors used to detect muons are called muon chambers. These chambers are multi-wire

proportional chambers. They have six planes of cathode strips slightly separated from anode wires immersed in a gas mixture of argon, carbon dioxide, and carbon tetra fluoride. When a muon, or any other charged particle, passes through the chamber, it ionizes the gas atoms. Because there is a high potential difference between the cathodes and wires (about four kilovolts), the positive ions and released electrons will drift to the oppositely charged electrode. When the electrons approach a wire, the electric field intensifies and the electrons accelerate. This causes the electrons to ionize more gas atoms, and the process repeats itself. This process eventually creates a large number of charged particles, thus magnifying the initial ionization by a factor of ~10^5 or more. When the electrons reach the wire, a pulse of current is detected by the electronics of the chamber. This process is referred to as an avalanche.

Objective

The performance of Cathode Strip Chambers (CSCs) in the CMS Endcap Muon System is related to the composition of the gas inside the chamber. The purpose of this experiment was to examine differences in the performance of CSCs under various mixtures of argon, carbon dioxide, and carbon tetrafluoride. The parameters of interest for each mixture are gas gain and operational voltage range, which were determined by measuring current from the cathode strips and count rates from the anode wires, respectively.

Gas Mixtures

The components of the gas mixtures were chosen according to properties that make them useful in multiwire proportional counters. Argon is inexpensive and helps to lower the voltage at which the chamber operates. Carbon dioxide is also inexpensive and is included to stabilize operation by minimizing spurious pulses through the absorption of photons (quenching). More

complicated organic molecules, e.g. C_4H_{10}, are even better quenchers, but their tendency to polymerize makes them undesirable. Carbon tetrafluoride also acts as a quencher, but it is included primarily because it is known to prevent aging in wire chambers. Unfortunately, it is expensive and may also corrode or etch chamber components if used in large quantities.

It was necessary to intuitively choose an appropriate "baseline mixture" as a starting point for the study. An Ar concentration of 40% allows for chamber operation at 3.6 kV, which is the default HV at which the chambers will operate at LHC. A CF_4 concentration of 10% was shown to prevent aging, does not appear to damage the chamber, and keeps the cost of the gas at reasonable levels. A mixture of Ar + CO_2 + CF_4 = 40 + 50 + 10 was therefore chosen as the base mixture. Other mixtures were selected for study by varying CF_4 concentration and Ar concentration with respect to the baseline mixture.

The nine gas mixtures used in the experiment are given in the following list and in Table I.

Ar + CO_2 + CF_4 = 40 + 50 + 10

40 + 60 + 0
40 + 55 + 5
40 + 45 + 15
40 + 40 + 20

20 + 70 + 10
30 + 60 + 10
50 + 40 + 10
60 + 30 + 10

Gas Mixtures Studied

% Ar \ % CF_4	0	5	10	15	20
60			X		
50			X		
40	X	X	**X**	X	X
30			X		
20			X		
10					
0					

TABLE I. The marked boxes indicate gas compositions included in the study. The gas mixtures are identified by Ar concentration and CF_4 concentration. The remaining portions of the mixtures consist of CO_2.

We combined the individual gases using a mechanical mixing device controlled by flowmeters for each of the three gases. We calibrated the flowmeters by using a stopwatch to measure the time for a soap bubble to travel a specified volume in a graduated cylinder for several flowmeter settings. The gas mixtures were delivered to the chamber at a flow rate of 400 cc/min.

Principal sources of error in the gas concentrations are instability in the flowmeter setting and human errors in timing and in volume readings from the graduated cylinder during flowmeter calibration. In addition, we discovered a unit conversion error in the CF_4 calibration after a substantial amount of data had been taken. However, we determined that the resulting uncertainty in CF_4 concentration was no more than 0.5%. Overall, the Ar and CO_2 concentrations are accurate to within 2%, while the CF_4 concentration is accurate to within 1%.

Procedure

We performed all tests using an ME2/1 prototype chamber. To determine the operational voltage range for each gas mixture, we measured count rates from the Anode Local Charged Track (ALCT) for voltages between 3.000 kV and 3.950 kV at steps of 50 V using the customized Data Acquisition System (DAQ) designed for the CSCs. The DAQ charge threshold was set at 20 fC, while the two-pulse time resolution was 300 ns. A Bertan Model 377 High Voltage Power Supply served as a voltage source, and we monitored voltage levels with a Fluke 85 Series III Multimeter. We performed six runs of count rate measurements at each voltage; each of these runs had a duration of 10 seconds. We then recorded the average of the six runs.

Measurements were first taken with the ALCT set to trigger when only one of the six anode planes registered a hit, generating a picture of the background rate. Cosmic ray count rates were found by setting the ALCT to trigger when four of the six anode planes registered hit patterns consistent with a particle trajectory, thereby ensuring that the DAQ recorded only charged particles passing through the detector and not random background events. A Cs-137 radioactive source was then placed on top of the chamber, and the count rates were again measured with the ALCT set to trigger at 1/6 and 4/6.

To determine gas gain, we measured currents from the cathode planes using a Kiethley 6485 Picoammeter. The current in each of the six cathode planes was recorded, also at voltages between 3.000 kV and 3.950 kV with 50 V steps. The currents were recorded with and without the Cs-137 source on the chamber.

Results: Gas Gain

The averages of the six cathode plane currents measured with the Cs-137 source present were plotted on semi-log axes. Low current values (below 10 nA) were discarded because the picoammeter had a nonzero offset of ~2 nA and its precision was not better than ~1 nA. Current values above 100 nA were discarded because the onset of spurious pulses at high voltages causes the right end of the curve to tail off. Gases with varying CF_4 content are shown in Fig. 1, while gases with varying Ar content are given in Fig. 2. In general, one can see from Fig. 1 that gas gain is essentially constant with respect to changes in CF_4 concentration. As expected, Fig. 2 shows that changes in Ar concentration have a significant effect on gas gain.

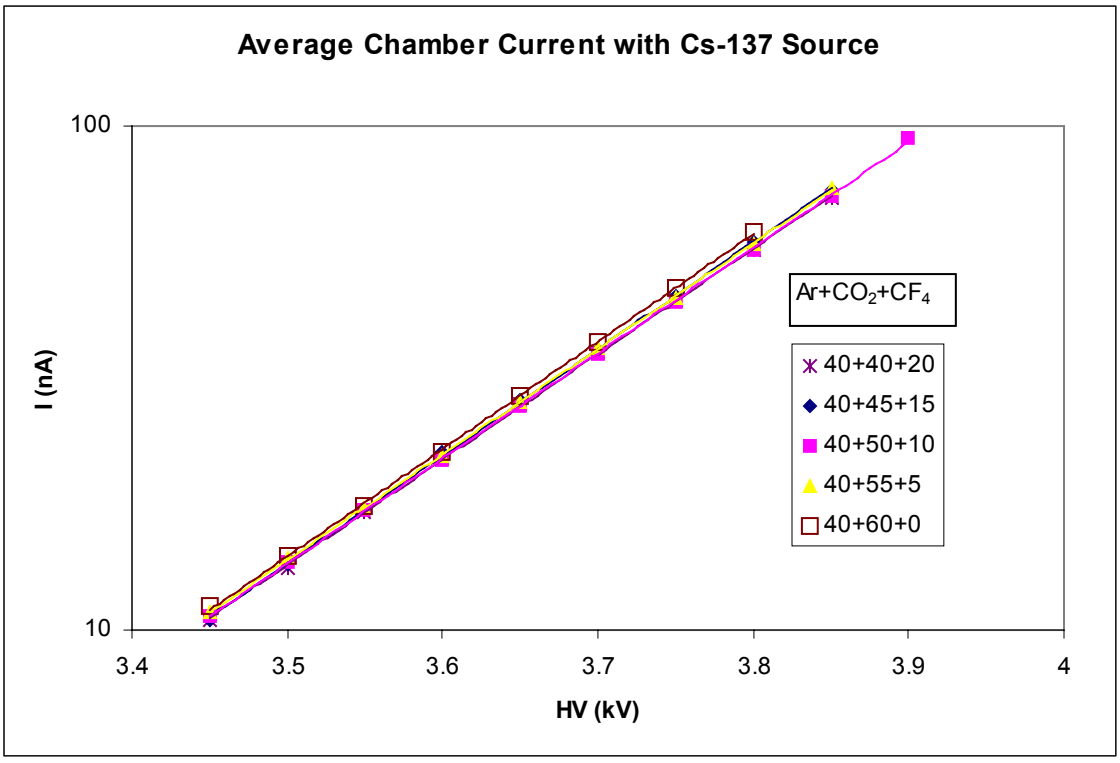

FIG. 1. Average cathode strip currents between 10 nA and 100 nA vs. HV for gases with varying CF_4 concentration.

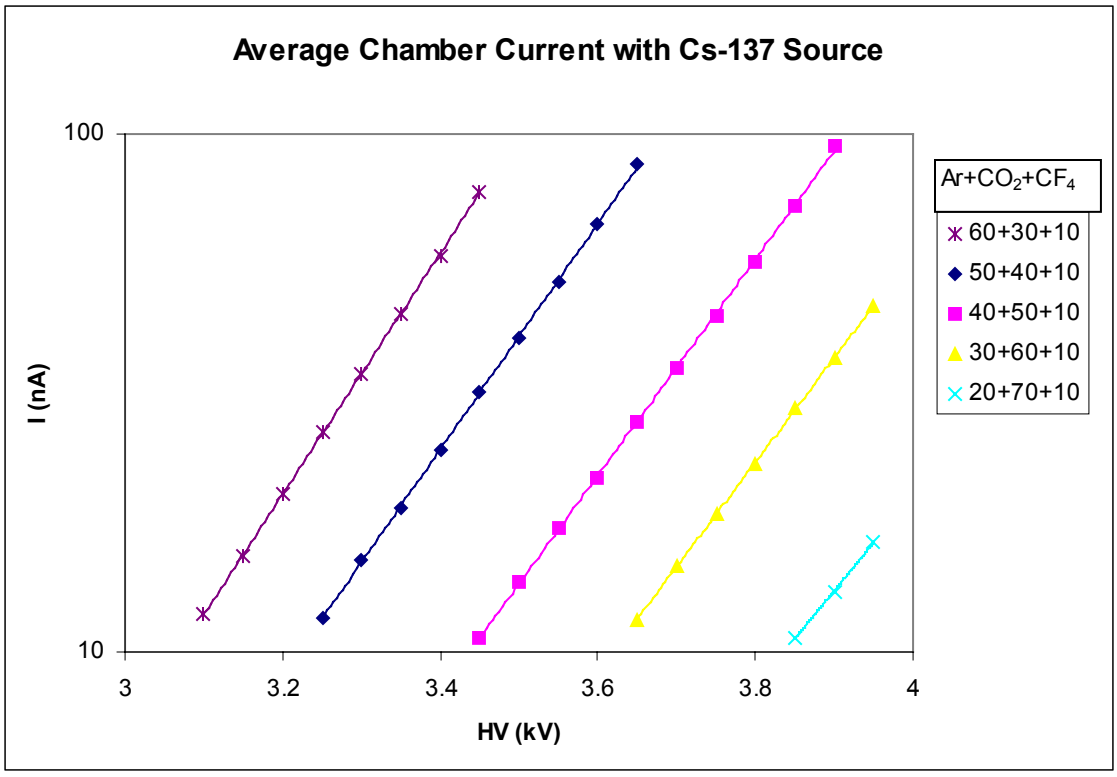

FIG. 2. Average cathode strip currents between 10 nA and 100 nA vs. HV for gases with varying Ar concentration.

The slope of the line through the data points for each gas (designated as α) characterizes how fast gas gain changes with high voltage: $G = G_0 \exp(\alpha \cdot \Delta V)$. Table II gives a summary of α values for each gas. Changes in CF_4 concentration have no significant effect, but gas gain is dependent on Ar concentration. We calculated error in α by plotting the α values for gases with varying Ar content and then finding the largest deviation from the regression line (see Fig. 3). We found the α values to be accurate to 0.09 kV^{-1}.

Gas Gain Slope α (kV^{-1})

% Ar \ % CF_4	0	5	10	15	20
60			5.36		
50			5.02		
40	4.91	4.82	4.79	4.89	4.82
30			4.64		
20			4.26		
10					
0					

TABLE II. α values for each gas mixture. Values are accurate to 0.09 kV^{-1}.

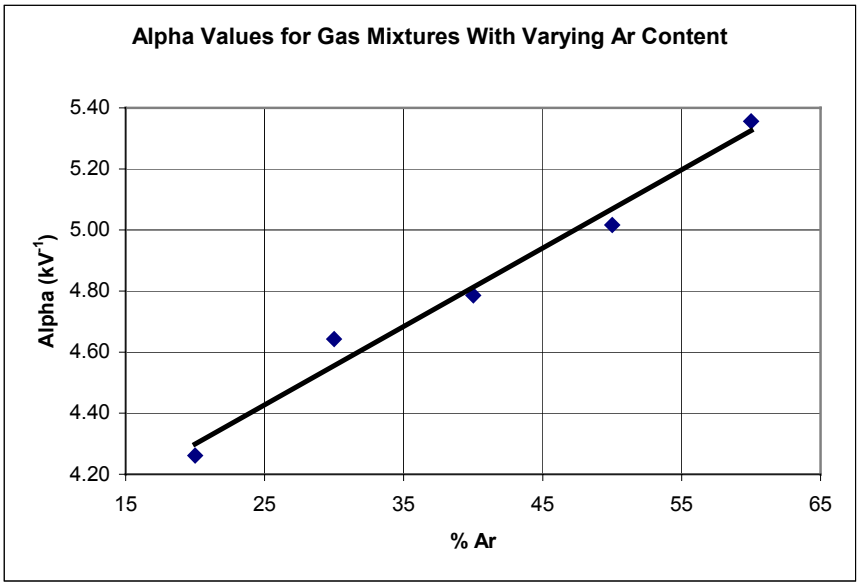

FIG. 3. α value vs. % Ar for the five gases with different Ar concentrations. The gas Ar + CO_2 + CF_4 = 30 + 60 + 10 has the largest deviation from the regression line (0.09 kV^{-1}), which we took to be the error in α.

Another measure of gas gain is HV needed to have a fixed gas gain (fixed current in our measurements). From the regression lines through the points in Fig. 1 and Fig. 2, it is possible to determine the voltage at which the average current is 20 nA. This current corresponds to the gas gain at the default 3.6 kV operation point of the baseline gas mixture (~10^5). The results are given in Table III. We found these values to be accurate to within 0.04 kV using a method similar to the method used to find the error in α.

HV at 20 nA Average Current (kV)

% Ar \ % CF_4	0	5	10	15	20
60			3.21		
50			3.35		
40	3.56	3.59	3.59	3.58	3.60
30			3.77		
20			4.00		
10					
0					

TABLE III. Voltages at which the average current is 20 nA for each gas mixture. Values are accurate to within 0.04 kV.

Again, gas gain is shown to be affected by Ar concentration but not by CF_4 concentration.

Results: Operational Voltage Range

Operational voltage range ΔHV is defined as the range of voltages at which the chamber operates at full efficiency and does not produce too many spurious pulses. The lower limit of ΔHV is determined by the voltage required to cause the chamber to detect all charged particles, while the upper end of ΔHV is determined by the onset of spurious pulses caused by unquenched photons in the chamber. Both ends of ΔHV are found by analyzing count rates.

The count rate is a measure of the number of particles detected by the chamber per second and is given in units of Hertz. There are two types of count rate measurements. The first type is taken with the ALCT set to trigger when any one out of the six anode planes registers a hit. These "singles" measurements are referred to as the background rate because they can be caused by anything from natural radioactivity to electronic noise in the chamber; these measurements are used to determine the upper limit of ΔHV (see below). The second type of measurement is taken with the ALCT set to trigger when four of the six planes along a possible particle trajectory register a hit. This process filters out the detection of everything other than charged particles moving through the detector. In this experiment, even when a radioactive source is present, the only source of charged particles is cosmic rays; hence, the 4/6 count rates are referred to as cosmic ray count rates. These cosmic ray count rates are used to determine the lower limit of ΔHV (see further below).

Fig. 4 shows cosmic ray count rates for three of the gases with different CF_4 concentrations; the other two gases are omitted for clarity in the graph, but they follow similar curves. Note that the curves "flatten out" above HV = 3.5 kV and form a plateau corresponding to 100% efficiency. This plateau occurs at approximately the same voltage for all of the gases in Fig. 3. The count rate at the plateau has an approximate value of 126 Hz.

Fig. 5 is a similar plot of cosmic ray count rates, but shows gases with varying Ar concentrations. The plateaus occur at different voltages, but the count rate at the plateau is

unaffected; it is again about 126 Hz for all gases, indicating no loss of efficiency due to changing Ar concentration.

Background count rates for gas mixtures with differing CF_4 concentrations are shown in Fig. 6. A plateau is evident in Fig. 6, but the curve has the additional feature of a tail at high voltages caused by spurious pulses; the location of the beginning of this tail is indicative of the upper limit of the operational voltage range. One can see that lower CF_4 concentrations cause spurious pulses to occur at slightly lower voltages. There is a considerable difference in the upper limit of ΔHV between the 40+60+0 and 40+50+10 mixtures, but the difference between the 40+50+10 and 40+40+20 mixtures is less prominent. This phenomenon suggests that the quenching abilities of CF4 are significant. When no CF4 is present, only CO2 acts as a quencher, thereby decreasing the number of photon wavelengths that can be absorbed.

The same plot for gases with varying Ar concentrations is shown in Fig. 7; in this case, it is clear that the plateaus for gases with higher Ar content end at lower voltages. The ends of the plateaus for the two gases with low argon content occur above 3.950 kV.

Figs. 8 and 9 show data similar to the data portrayed in Figs. 6 and 7, with the exception that the count rates in Figs. 8 and 9 were obtained with the Cs-137 source in place. Although the count rate values are different, the ends of the plateaus in Figs. 8 and 9 occur at the same voltages as in Figs. 6 and 7.

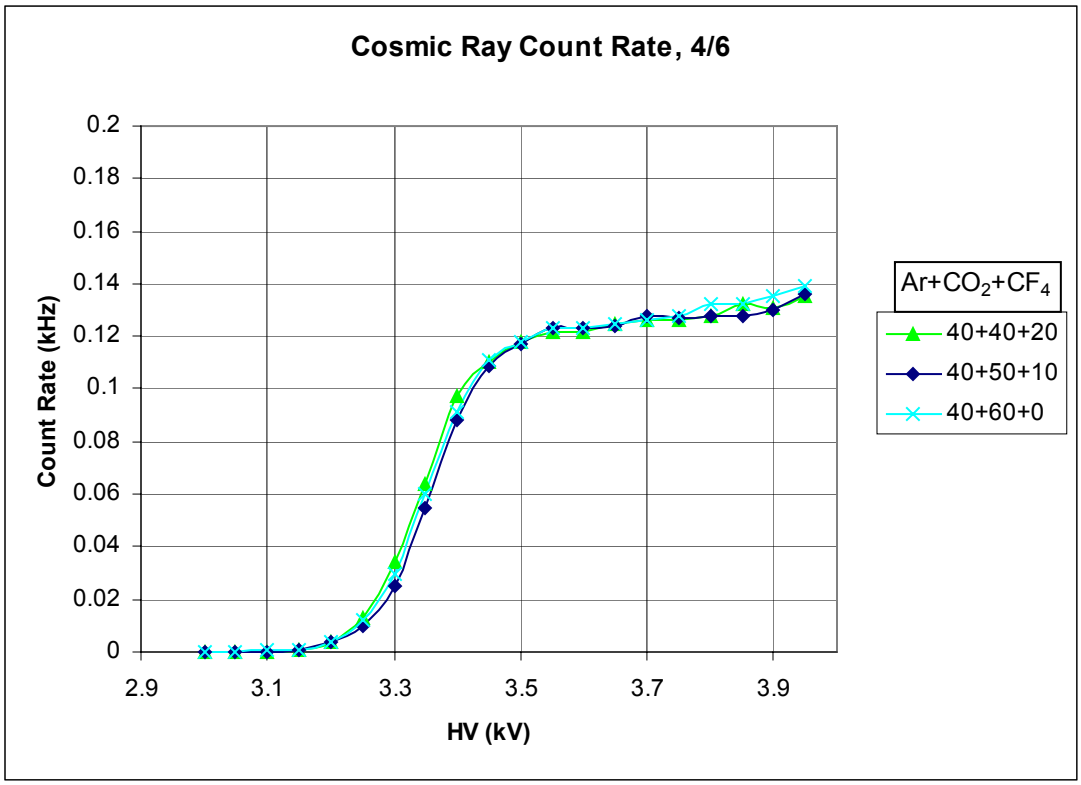

FIG. 4. Cosmic ray count rate vs. HV for gases with varying CF_4 concentrations.

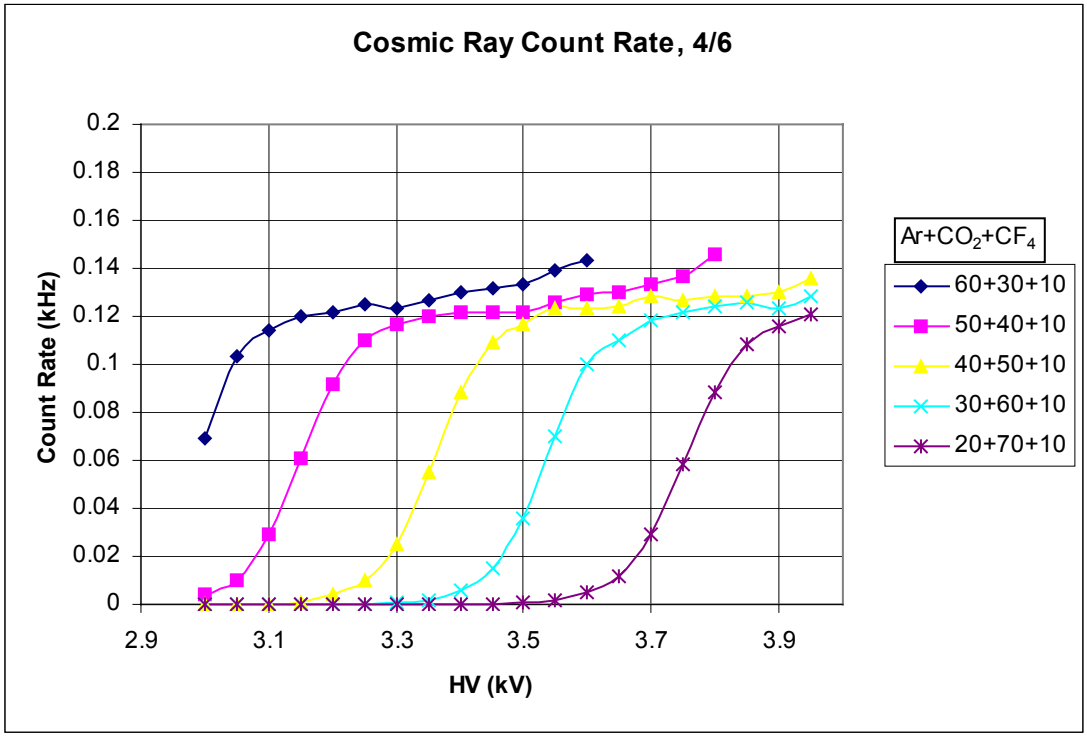

FIG. 5. Cosmic ray count rate vs. HV for gases with varying CF_4 concentrations.

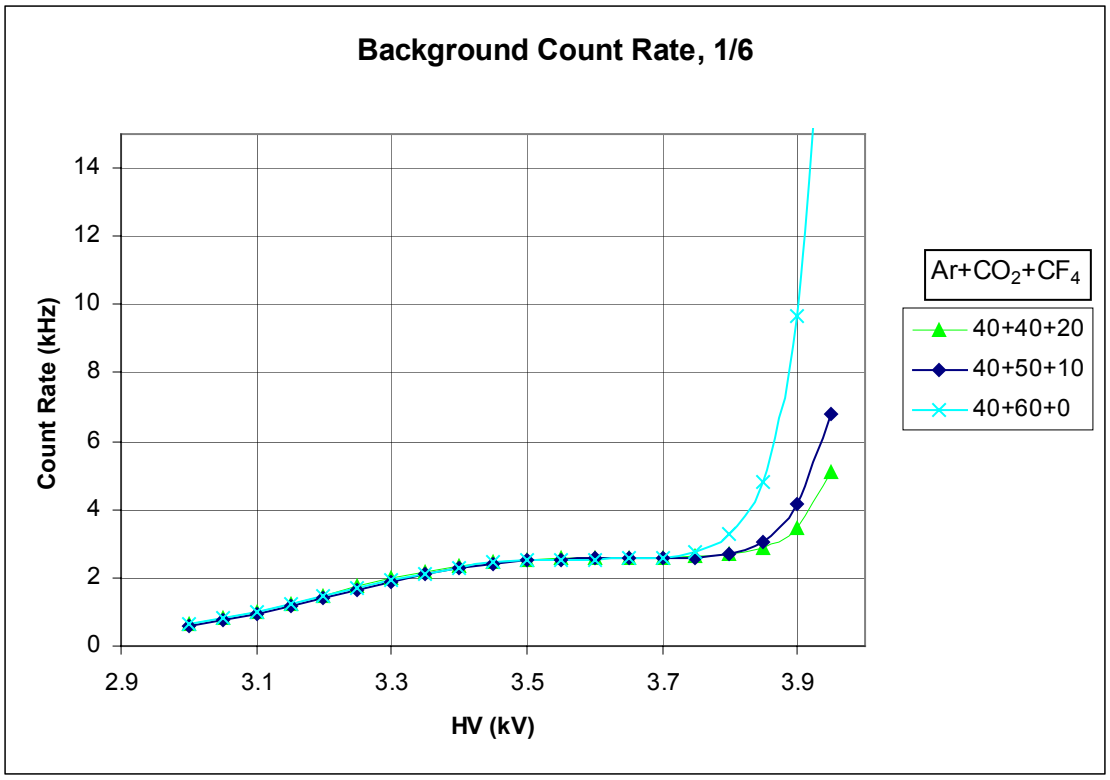

FIG. 6. Background count rate vs. HV for gases with varying CF_4 concentrations.

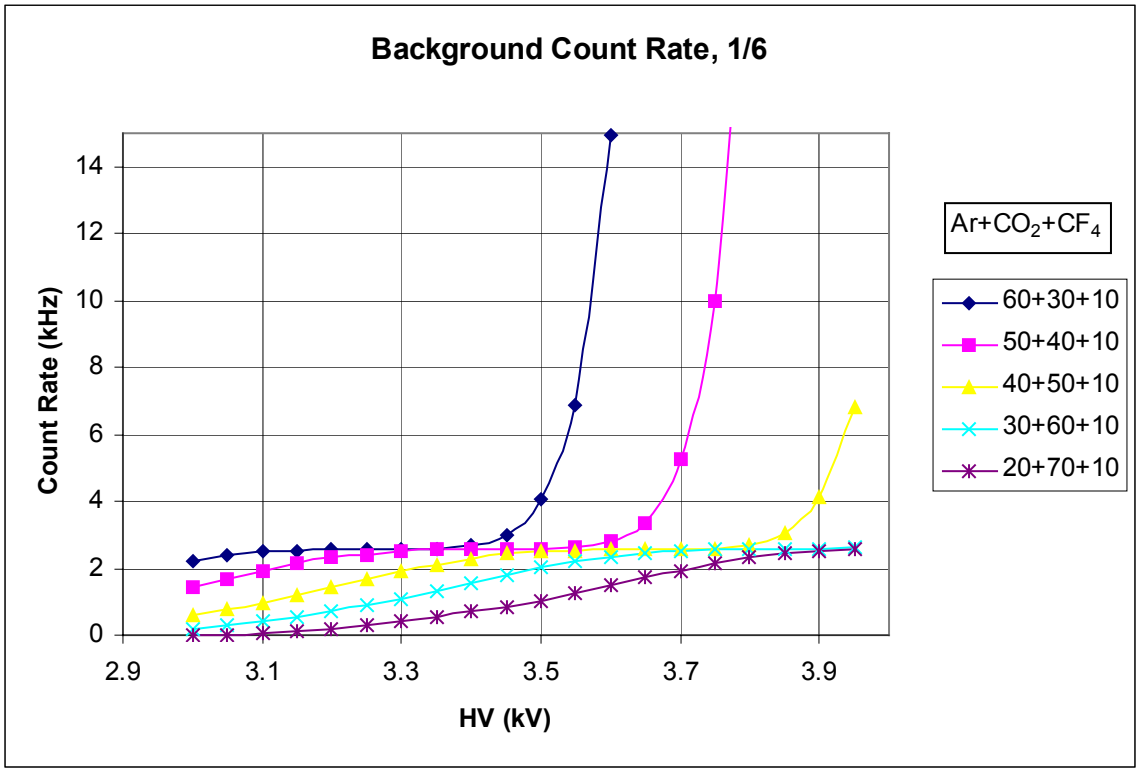

FIG. 7. Background count rate vs. HV for gases with varying Ar concentrations.

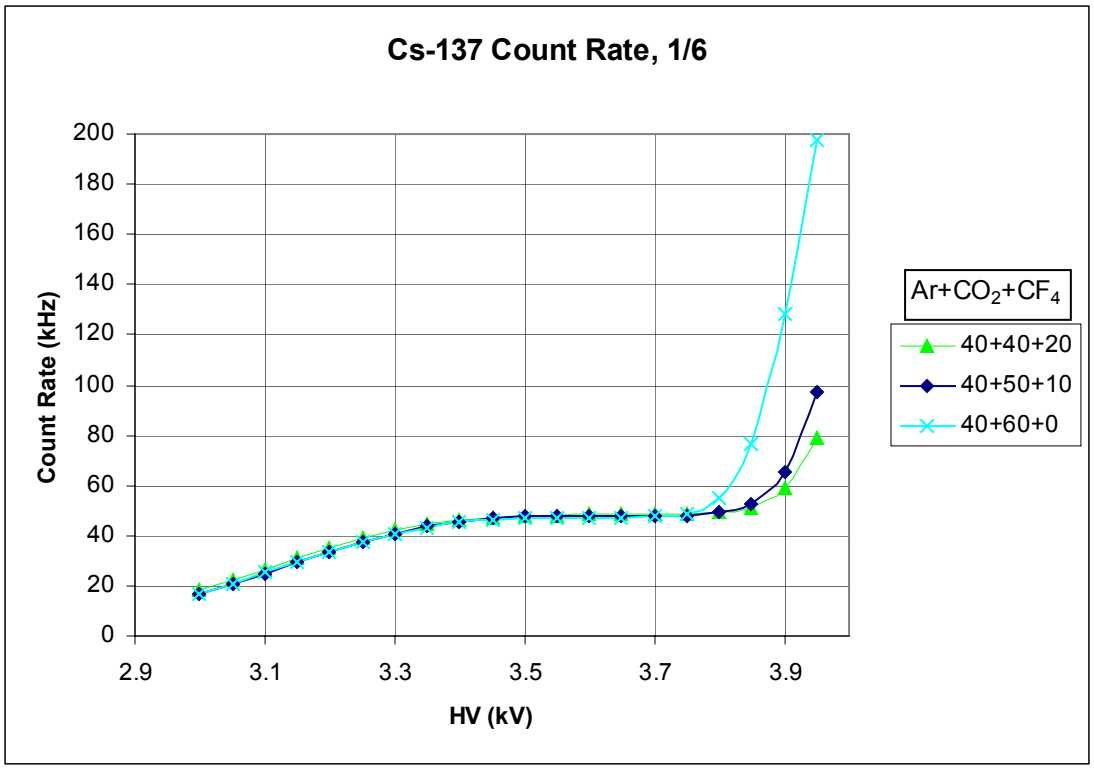

FIG. 8. Cs-137 count rate vs. HV for gases with varying CF_4 concentrations.

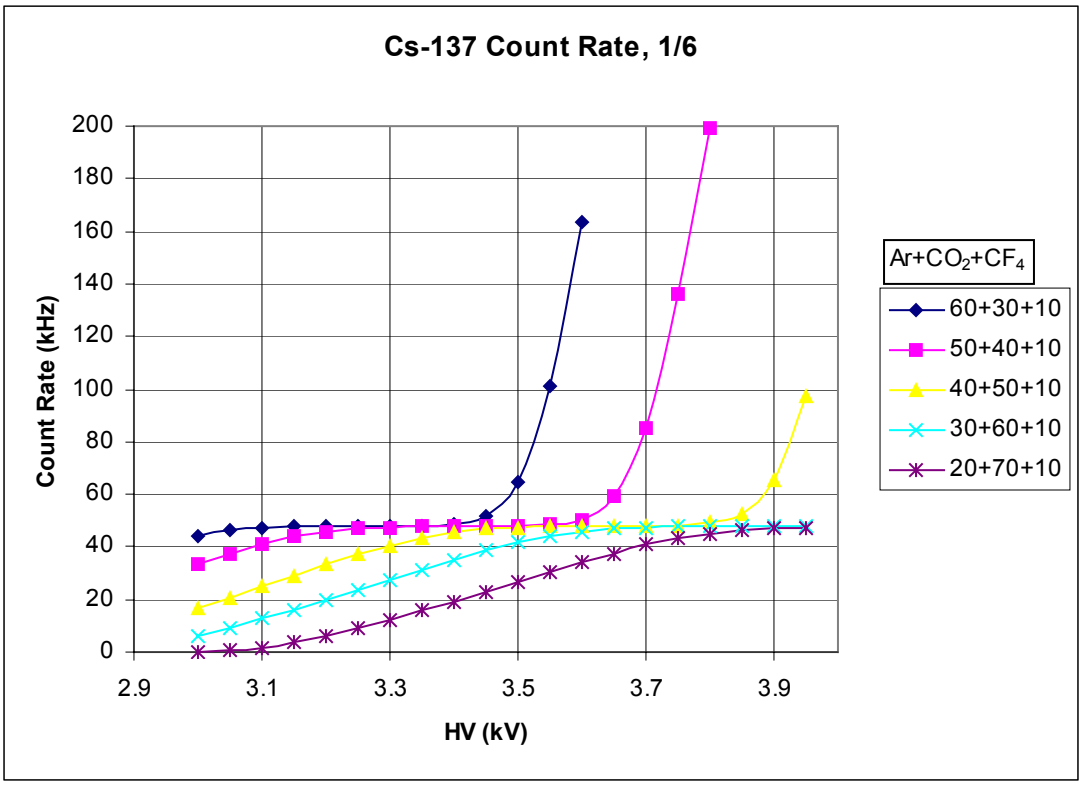

FIG. 9. Cs-137 count rate vs. HV for gases with varying Ar concentrations

An indication of the start of the operational voltage range can be obtained from Figs. 4 and 5. The curves are fast rising and approximately linear around the 50% efficiency mark; consequently, a linear fit using the points around this mark can be used to accurately determine the voltage at which the efficiency is 50%. Because the plateau count rate is approximately 126 Hz, we defined the 50% efficiency point as 63 Hz. Voltages at which the count rate is ~63 Hz are given in Table IV. It is evident that changes in CF_4 concentration have a minimal effect on the location of the start of the plateau, while changes in Ar concentration have a significant impact. This conclusion is consistent with the results of the gas gain analysis.

HV at 50% Efficiency, 4/6 (kV)

% Ar \ % CF_4	0	5	10	15	20
60			2.99		
50			3.15		
40	3.35	3.36	3.37	3.35	3.35
30			3.54		
20			3.76		
10					
0					

TABLE IV. Voltages at which the cosmic ray count rate is 50% of the plateau count rate. Values are accurate to within 0.04 kV.

The HV at which the chamber becomes ~100% efficient is about 150 V higher than the point of 50% efficiency (see Figs. 4, 5). Thus, we chose to use HV(50% eff.) + 150 V as the voltage corresponding to full chamber efficiency.

Figs. 8 and 9 were used to determine the upper limit of the operational voltage range. We defined the end of the plateau as the point at which spurious pulses cause the count rate to be 50% above the plateau count rate. Because the plateau count rate is ~48 kHz, the point at which the count rate is 50% above the plateau is ~71 kHz. We constructed a linear fit using selected

data points above the plateau to find the voltages at which the count rate was ~71 kHz. The results are given in Table V. The location of the end of the plateau is only slightly affected by changes in CF_4 concentration, but it varies significantly with changes in Ar concentration.

HV at End of Plateau, 1/6 (kV)

%Ar	0	5	10	15	20
60			3.51		
50			3.67		
40	3.84	3.90	3.91	3.90	3.93
30			> 3.95		
20			> 3.95		
10					
0					

$\%CF_4$

TABLE V. Voltages at which the count rate is 50% above the plateau count rate due to spurious pulses. The voltages were determined from data taken with the Cs-137 source on the chamber. Values are accurate to within 0.04 kV.

The difference between the HV at the starting point of full chamber efficiency and the HV at the end of the plateau gives ΔHV, the operational voltage range; the results are given in Table VI.

Operational HV Range (kV)

% Ar	0	5	10	15	20
60			0.37		
50			0.37		
40	0.34	0.39	0.39	0.40	0.43
30			N/A		
20			N/A		
10					
0					

$\%\ CF_4$

TABLE VI. Operational HV ranges for different gas mixtures. Values are accurate to within 0.04 kV.

No significant increase in operational range can be expected by altering the concentration of Ar between 40% and 60%. There is an increase in ΔHV between the 0% CF_4 and 20% CF_4 mixtures. However, the largest change in ΔHV occurs between the 0% CF_4 and 5% CF_4 mixtures (~50 V). This phenomenon may be attributed to the quenching abilities of CF_4; when CF_4 is present, the number of photon wavelengths that can be absorbed is increased, thus delaying the onset of spurious pulses and increasing ΔHV. The increase in ΔHV between the 5% and 20% CF_4 mixtures is much more gradual and can even be considered negligible when error is accounted for.

Conclusions

The performance of a prototype cathode strip chamber was tested under gas mixtures with varying Ar and CF_4 concentrations around the baseline point of Ar + CO_2 + CF_4 = 40 + 50 + 10. An increase in the concentration of Ar up to 60% causes a decrease in operational HV without decreasing the range of operation ΔHV. An increase or decrease in the concentration of CF_4 (0-20%) has a negligible effect on gas gain. The absence of CF4 causes a slight drop in ΔHV, but once CF_4 is present, there is no significant change in ΔHV with respect to changing CF_4 concentration. The data suggest that the gas mixture Ar + CO_2 + CF_4 = 60 + 35 + 5 is optimal because of the low operational voltage and low cost that it offers, provided that further studies show that 5% CF_4 is sufficient to prevent premature aging.

Acknowledgements

The authors wish to thank Dr. Kevin Ingersent, Dr. Alan Dorsey, Donna Balkcom, and Shawn Allgeier for organizing and overseeing the University of Florida's Physics Research

Experience for Undergraduates (REU) program. We are also grateful for the National Science Foundation's sponsorship of the REU program, without which this project would not have been possible.